SIN-CHN SCIENTIFIC PRESS PTE.LTD.

Molecular & Cellular Biomechanics 2025, 22(4), 1451.
https://doi.org/10.62617/mcb1451

Article

Influence of dynamic monitoring of blood routine indexes on ECG characteristics of elderly patients with diabetes and the application of sensor technology

Lisha Zhang[1], Yan Yang[2], Ning Ma[3,*]

[1] Rest House Outpatient Department, Outpatient Department of the 18th Retired Cadre Nursing Home in Haidian District, Beijing Garrison, No. 8-37 Huayuan East Road, Haidian District, Beijing 100191, China
[2] Physical Examination Center Medical, Suzhou Industrial Park Jiatai Outpatient Department Co., Ltd, C114, South Annex Building, Huihu Building, No. 10 Moon Bay Road, Suzhou Industrial Park, Suzhou 215100, China
[3] Rest House Outpatient Department, Outpatient Department of Changping Retired Cadres Rest House in Beijing Garrison District, Yifeng Garden, Dongxiaokou Town, Changping District, Beijing 100096, China
*** Corresponding author:** Ning Ma, Maningzaibeijing@163.com

CITATION

Zhang L, Yang Y, Ma N. Influence of dynamic monitoring of blood routine indexes on ECG characteristics of elderly patients with diabetes and the application of sensor technology. Molecular & Cellular Biomechanics. 2025; 22(4): 1451. https://doi.org/10.62617/mcb1451

ARTICLE INFO

Received: 24 January 2025
Accepted: 17 February 2025
Available online: 12 March 2025

Abstract: To provide a more efficient and real-time blood routine monitoring method for elderly patients with diabetes, and to explore the correlation between blood routine indexes and Electrocardiogram (ECG) characteristics. A real-time blood routine detection device based on electrochemical sensor was designed, and a portable instrument based on optical sensor was developed to monitor trace biomarkers in blood using a labeled electrochemical biogold nanoparticle sensor. The results show that the sensor can monitor bilirubin level in real time, and the correlation coefficient with blood routine results is 0.95, so that the clinical monitoring time is shortened from 2 h to 30 min. The detection limit of white blood cell count was 0.85 × 10^9/L, and the data collection rate was 50 times/s, which improved the detection accuracy by 15.8% compared with the traditional laboratory method. In addition, the study revealed the mechanism of potential influence of changes in blood routine indicators on ECG characteristics. The monitoring device in this study can reduce the cost, improve the efficiency, and provide a precise and convenient clinical application scheme for the health management of elderly diabetes patients.

Keywords: geriatric diabetes mellitus; electrocardiographic features; routine blood markers; bilirubin sensor; real-time monitoring

1. Introduction

Diabetes mellitus is one of the common and serious metabolic diseases in the elderly, with high morbidity and disability rates that require attention and effective monitoring. Early diagnosis and intervention are essential to improve the prognosis of patients. In recent years, α2-macroglobulin (α2-M) has received widespread attention as a potential biomarker for diabetes [1]. It has been found that the concentration of α2-M in the serum of diabetic patients is significantly higher than that of the healthy population, and the level of its changes is closely related to the onset and progression of diabetes mellitus, making it a potential early diagnostic marker [2]. In addition, bilirubin, as an erythrocyte metabolite, has attracted much attention for its antioxidant properties in diabetic patients. Abnormal bilirubin levels are strongly associated with inflammation, oxidative stress, and cardiovascular complications, especially in elderly patients. It can provide key clues for disease monitoring and risk assessment [3]. The interaction between diabetes mellitus and the cardiovascular system is particularly

evident through electrocardiographic features. The electrocardiograms of patients with geriatric diabetes mellitus usually show prolonged QRS and T (QT) intervals, T-wave abnormalities, and ST-segment changes. The increasing number of diabetic patients has promoted the development of glucose sensor technology, especially the potential of electrochemical biosensors in dynamically monitoring blood glucose. These features are closely related to fluctuations in blood glucose levels, inflammatory responses, and electrolyte imbalances. Dynamic monitoring of changes in blood markers can provide early warning signals for Electrocardiogram (ECG) abnormalities, leading to better identification of cardiovascular risks [4].

In recent years, the monitoring and sensing technology of blood indicators in diabetic patients has made progress, but there are still gaps. Studies focused on a single biomarker and lacked multi-indicator dynamic monitoring in elderly patients. Although α2-macroglobulin and bilirubin are closely related to diabetes, there is still a lack of efficient real-time detection technology. In addition, optical biosensors are vulnerable to environmental influences, real-time glucose monitoring depends on the accuracy of the equipment, and the early warning system needs to be optimized. Studies on the regulatory mechanism of nutritional sensors are insufficient, especially in elderly patients, and their effects on blood index changes and electrocardiogram characteristics need to be explored. To fill these gaps, the study constructs a highly sensitive electrochemical biosensor by layer-by-layer self-assembly technique, which utilizes the synergistic effect of gold nanoparticles (AuNPs) and capture probes to achieve efficient detection of micro ribonucleic acid (microRNA, miRNA). Next, the sensor's ability to specifically recognize biomarkers such as α2-M is enhanced by the synergistic effect of antibody modification and key proteins. In addition, the dynamic monitoring of electrocardiographic features combined with the application of biosensor technology provides a powerful support for personalized diagnosis and prediction of complications in geriatric diabetes mellitus patients. This study aims to develop a real-time monitoring system for blood routine indexes in elderly diabetic patients and investigate their correlation with ECG characteristics using advanced sensor technology.

2. Related works

As the number of diabetic patients increases year by year, more and more researchers have begun to pay extensive attention to the study of changes in blood indicators of diabetes and the application of sensor monitoring technology. Sani et al. [5] proposed a two-dimensional photonic crystal optical biosensor method based on a resonant cavity for high-precision detection of biological samples. The results showed that the sensor was able to detect diseases by analyzing blood, urine and tear samples with a sensitivity of up to 10,000 nm/RIU and an optimal value of 48,543 RIU-1 for the performance index. While Sani et al. [5] demonstrated high sensitivity in optical biosensors, our study aims to improve upon their work by incorporating real-time monitoring capabilities. Marigliano et al. [6] addressed the issue of hypoglycemic events in adolescents with type 1 diabetes mellitus (AwD) by proposing the use of Real-Time Continuous Glucose Monitoring (RT-CGM) method with predictive alarms. The results showed a significant reduction in the time spent

in severe hypoglycemia and hypoglycemic states and an improvement in the quality of glycemic control in AwD using Predictive Alarm (PA.) Marigliano et al. [6] proposed a real-time continuous glucose monitoring approach, but our study further optimizes the early warning system and extends multi-indicator dynamic monitoring. Carol et al. [7] addressed the lack of a customized closed-loop insulin delivery system for pregnant patients with type 1 diabetes by proposing the use of a predictive Closed-Loop Predictive Control System (CLC-P) using a regional model customized for pregnancy. Results showed that home use of the CLC-P was feasible and significantly increased time to glucose attainment and reduced hyperglycemic and hypoglycemic events. Carol et al. [7] developed a closed-loop insulin delivery system, but our study provides a more comprehensive approach to diabetes management by incorporating ECG signature monitoring.

Lazar et al. [8] addressed the question of the mechanism of insulin secretion control in pancreatic *P*-cells and presented the important discovery of glucokinase as a glucose sensor, overturning the prevailing view at the time. The results showed that the findings were highly reproducible and were supported by biochemistry and murine and human genetics, laying the foundation of the field. Lazar et al. [8] discovered glucokinase as a glucose sensor, but our study further explores its use for dynamic monitoring in elderly patients with diabetes. Schiavon et al. [9] addressed the need to estimate insulin sensitivity and its daily variability for optimizing insulin therapy in patients with type 1 diabetes by proposing a method for estimating insulin sensitivity using continuous glucose monitoring and continuous subcutaneous insulin infusion data. The results showed that the study method had high estimation accuracy, was highly correlated with the gold standard, and was suitable for both closed-loop and open-loop settings. Schiavon et al. [9] proposed an insulin sensitivity estimation method, but our study provided a more accurate personalized diagnosis by combining the monitoring of blood routine indicators. Riahi et al. [10] proposed to study the regulatory role of the nutrient sensor in alpha cells in response to the dysfunction of alpha cells in diabetes that leads to dysregulation of glucagon secretion. The results showed that hyperglycemia could enhance amino acid synthesis and transport, sustained activation of this sensor, and increased glucagon secretion. The research methodology was confirmed to play a major role in diabetic α-cell dysfunction. Riahi et al. [10] investigated the role of nutritional sensors in diabetes, but our study further explored its impact on ECG characteristics.

Although some progress has been made in the above studies, there are still limitations. For example, optical biosensors, although highly sensitive, may be affected by the sample preparation and measurement environment. The RT-CGM method relies on the accuracy of the device and the early warning system needs to be further optimized. The CLC-P system needs more clinical validation. Sensor methods may be affected by individual differences in practical application. Most of the studies need to explore the regulatory mechanisms of nutrient sensors in depth. Therefore, the new label-free electrochemical bio-AuNP sensor designed for the study aims to improve the efficiency of monitoring blood and cardiac characteristics in geriatric diabetes mellitus patients. Its effectiveness in real samples is also validated to overcome the shortcomings of existing studies.

3. Experimental materials and method

3.1. Experimental materials

The main reagents used in the preparation of label-free electrochemical bio-AuNP sensors and in the experiments for monitoring routine blood indicators in the elderly are shown in **Table 1**.

Table 1. Experimental reagents and sources.

Reagent name	Supplier	Reagent name	Supplier
Polydimethylsiloxane (PDMS)	Zhuhai Kelibang technology Co., Limited (LTD)	Bovine Serum albumin (BSA)	Shanghai Macklin Biochemical Technology Co., LTD
Manganese ferrite ($MnFe_2O_4$)	Guangzhou and for medical technology Co., LTD	1. Ethyl-3-(3-dimethylaminopropyl) carbodiethylene	Beijing MREDA Technology Co., LTD
Chitosan (CS)	Beijing Sinopharm Co. LTD	Amine hydrochloride (EDC)	Beijing MREDA Technology Co., LTD
PCR related reagent	Thermo scientific	N-hydroxysulfosuccinimide (NHS)	Shanghai Chengong Biotechnology Co., LTD
Bilirubin oxidase (BOD)	Synthetic/commercial kits	a2 macroglobulin (u2-M)	Shanghai Chengong Biotechnology Co., LTD
Near-infrared Fluorescent Protein (BDFP1.6)	Synthetic/commercial kits	a2-MG	Shanghai Macklin Biochemical Technology Co., LTD
Lysozyme (LYZ)	Shanghai Chengong Biotechnology Co., LTD	Human Serum albumin (HSA)	Shanghai Chengong Biotechnology Co., LTD
C-reactive protein (CRP)	Shanghai Chengong Biotechnology Co., LTD	uric acid	Shanghai Chengong Biotechnology Co., LTD

The main apparatus used for the experiment is shown in **Table 2**.

Table 2. Experimental instruments and sources.

Instrument name	Supplier	Instrument name	Supplier
Hitachi HT7700 transmission electron microscope	JEOL LTD., Japan	HR-800 confocal Raman spectrometer	French JY Company
X-ray diffractometer	Panaco, Netherlands	*X*-ray photoelectron spectrometer	VG, UK
KQ-300DEC ultrasonic cleaning machine	Kunshan Ultrasonic Instrument Co., LTD	CHI 660D Electrochemical workstation	Shanghai Chenhua Instrument Co., LTD.
BPZ-6090 vacuum drying oven	Shanghai Yiheng Scientific Instrument Co., LTD	SIGMA-500 Scanning Electron Microscope (SEM)	Zeiss
KQ-250DE ultrasonic cleaning machine	Kunshan Ultrasonic Instrument Co., LTD	Pure water preparation machine	Xi'an Youpu instrument equipment company
Cubis-11 weighing balance	Germany Sartorius Aktiengesellschaft	Fourier infrared spectrometer (FTIR)	Tianjin Jingtuo instrument Technology Co., LTD
Integrated physical properties measurement system (PPMS)	Quantum Design, USA	Spin coating and glue spinner	Midas System, Korea
Pipette gun	Eppendorf, Germany	Digital source table	Guangzhou Meidac data Technology Co., LTD

3.2. Sensor fabrication

3.2.1. AuNP synthesis and preparation of electrochemical biosensors

The electrochemical biosensor was constructed by step-to-step modification.

AuNPs is synthesized by stirring 1 mL 1% HAuCl4 into 100 mL ultra-pure water and heating it to a boil. Quickly add 10 mL 1% sodium citrate solution and continue stirring for 15 min until the solution changes from light yellow to dark red, indicating AuNPs formation. Cool to room temperature and store at 4 ℃ away from light.

The materials required for the preparation of the electrochemical biosensor are glassy carbon electrode Glassy Carbon Electrode (GCE), diameter 3 mm, ALS Co., Ltd.) and capture probe (5'-SH-(CH2) 6-AAAAAAA-3'). The preparation steps are as follows: The first step is electrode pretreatment. The GCE was polished with 0.3 μm and 0.05 μm aluminum oxide powder, rinsed with ultra-pure water, and ultrasonic cleaned in ethanol and ultra-pure water for 5 min, respectively. The second step is to prepare the FeCN/GCE electrode [11]. Add 10 μL 10 mm potassium ferricyanide solution to GCE, let it stand for 10 min, rinse with ultra-pure water to remove the unadsorbed matter. The third step is to prepare AuNP/FeCN/GCE electrodes. Drop 10 μL AuNPs solution to FeCN/GCE, stand for 30 min, rinse with ultra-pure water to remove unadsorbed AuNPs. Step four, fix the capture probe. The 50 μm trapping probe was mixed with 50 μm TCEP and reacted at room temperature for 1 h to reduce the mercaptan group. 10 μL probe solution was added to AuNP/FeCN/GCE, incubated overnight at 4 ℃, and the unfixed probe was removed by rinsing with ultra-pure water. Finally, 10 μL of 1 mm MCH solution was added to the electrode surface and incubated at room temperature for 1 h to seal the unreacted AuNPs surface. Flush the electrode with ultra-pure water to remove unreacted Mercaptohexanol (MCH).

3.2.2. Construction of miRNA electrochemical biosensor

Experiments were performed to construct miRNA electrochemical biosensors by DNA-RNA hybridization [12]. First, modified electrodes (MCH/capture probe/AuNP/FeCN/GCE) were incubated with different concentrations of miRNA at 37 ℃ for 2 h to complete hybridization and washed. Subsequently, the electrode was reacted with poly (A) polymerase and ATP in extension solution for 1 h for RNA strand extension, washed again, and exposed to T-rich auxiliary probes to form poly (T) complexes. After washing, the nonspecific adsorption was removed by dropwise incubation with thiosulfur at 37 ℃ for 1 h. Finally, the electrochemical signal response was detected by differential pulse voltammetry (DPV) in acetate buffer. The electrochemical biosensor was based on a layer-by-layer self-assembly technique. First, ferricyanide (FeCN) and AuNP were modified on the surface of the glassy carbon electrode, and the thiolated capture probe was immobilized by gold-sulfur bonding [13]. **Figure 1** shows the process of miRNA sensitively detected by the biosensor.

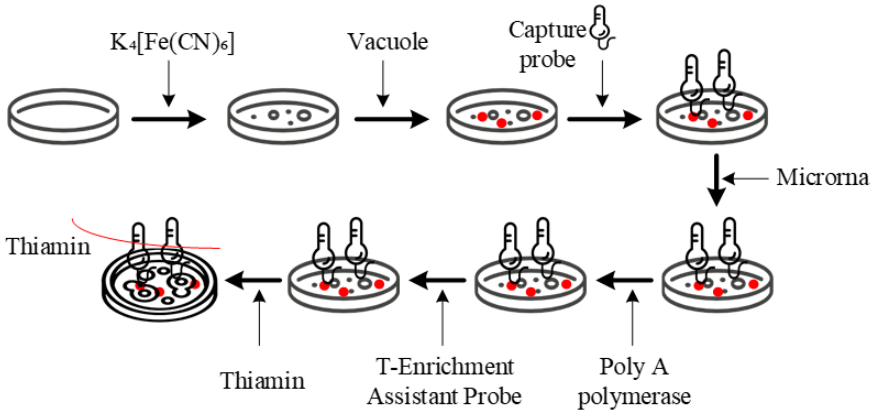

Figure 1. Process of miRNA sensitively detected by biosensors.

3.3. Detection methods

3.3.1. Methods of cellular serum analysis

Biosensors achieve highly specific recognition of α2-M molecules by modifying α2-M antibodies on their surfaces [14,15]. To enhance the binding effect of the antibody to the sensor surface, the antibody needs to be chemically modified, usually by synergistic treatment with NHS (N-hydroxysuccinimide) and EDC (1-ethyl-3-(3-dimethylaminopropyl) carbodiimide). This approach enhances the immobilization efficiency of the antibody on the sensor surface by activating specific groups on the antibody through the reaction between NHS and EDC. The modified antibody is firmly attached to the surface of the sensor through covalent bonds, ensuring its stable presence and specific recognition of α2-M in the sample solution. To reduce the non-specific binding between the antibody and other molecules, bovine serum albumin (BSA) is usually used to seal the unreacted active site [16]. This closure step effectively reduces background noise and improves the sensitivity and selectivity of the sensor. Subsequently, the processed sensor is placed in a sample solution containing α2-M. The specific binding of the antibody to the target molecule leads to a change in the structure of the sensor surface, which triggers a change in electrical resistance and magnetic permeability. This change stems from the molecular mechanical effects induced by antibody-antigen binding, which in turn have an impact on the electronic conductivity of the sensor surface. Quantitative detection of α2-M can be achieved by monitoring changes in sensor surface resistance and permeability in real time with an integrated physical property measurement system such as electrochemical impedance spectroscopy (EIS) or magnetic permeability analyzer.

The synergistic effect of three key proteins is required in sensor design in addition to the surface modification of the antibody: multidrug resistance-associated protein 2 (MRP2), bilirubin oxidase (BOD), and unagi-derived bilirubin-binding fluorescent protein (UnaG). These proteins play important roles in enhancing sensor functionality and signal amplification. MRP2, a transmembrane protein, is responsible for bilirubin transport and processing. The MRP2 gene is amplified by PCR and inserted into the pET28a plasmid using enzymatic digestion and ligation techniques to construct the pET28a-mrp2 recombinant plasmid. This plasmid can be transformed into E. coli BL21 to express MRP2 protein, which is subsequently purified using nickel chelate affinity chromatography to provide the basis for sensor functionalization. UnaG is a

novel fluorescent protein with the ability to bind bilirubin directly, making it an ideal component for bilirubin sensors. The UnaG gene is amplified by PCR and inserted into the pCDFDuet plasmid using enzymatic digestion and ligation to construct the pCDFDuet-unag recombinant plasmid. This plasmid is co-transformed with pET28a-mrp2 into E. coli BL21 to realize the co-expression of the two proteins. The fluorescent properties of UnaG significantly enhance the signal intensity in bilirubin assay. Cells with bilirubin sensing function are successfully constructed by co-transforming pET28a-mrp2 and pCDFDuet-unag plasmids. These cells can efficiently express MRP2 and UnaG proteins under suitable induction conditions, and subsequently purified to obtain high-purity proteins. Combining the bilirubin transmembrane transport function of MRP2 and the fluorescent signaling property of UnaG, the sensor can efficiently detect bilirubin.

3.3.2. Determination of spectra

Commonly used such as fourier transform infrared spectrometer (FTIR) is used to analyze chemical bonds and functional groups [17]. The instrument needs to be calibrated before measurement to ensure accurate data. The sample is placed correctly in the instrument and the appropriate measurement parameters such as wavelength range and resolution are set to obtain high quality data. A background scan is performed to eliminate interferences and the sample is subsequently scanned to record the spectral data. Whereas, fluorescence spectroscopy enables detection through the fluorescent signal emitted by fluorescent substances under the excitation of a specific light source. Human plasma samples are first collected and subjected to appropriate pretreatment such as centrifugation and filtration to remove impurities that may affect the fluorescence signal [18,19]. Then, suitable quantum dots are selected as fluorescent markers, which should have excellent signal brightness and photostability. The probe is contacted with the sample to be tested so that the aptamer on the probe binds specifically to the target protein, enabling it to specifically recognize the target biomarker. An antibody or aptamer labeled with quantum dots is mixed with the sample to be tested, allowing the quantum dots to bind specifically to the target biomarker. The fluorescence signal of the quantum dots is detected using a fluorescence spectrometer. The quantum dots are excited and the intensity of the fluorescence emitted is recorded.

For samples requiring protein spectroscopy, the cells need to be physically or chemically broken to release the internal proteins. The target proteins are then purified for spectroscopic determination by methods such as nickel ion affinity chromatography. Absorption spectra of samples in a specific wavelength range are determined using UV-Vis absorption spectroscopy [20]. For the bilirubin biosensor, special attention is paid to the characteristic absorption peak of bilirubin, about 450 nm, and the change in the absorption peak upon binding of bilirubin by fluorescent proteins. The sample is transferred to a fluorescence spectrometer to determine the fluorescence spectrum. Parameters such as excitation and emission wavelengths, scanning speed, slit width, and gain are set. For the biosensor, the excitation wavelength is set to 620 nm and the emission wavelength is set to 640 nm. After collecting the spectral data, the changes in absorption and fluorescence spectra are analyzed. For the absorption spectra, the differences in absorption peaks between the

experimental and control groups are compared. For the fluorescence spectra, the changes in fluorescence intensity at different bilirubin concentrations are compared to evaluate the responsiveness of the biosensor.

3.4. Statistical methods

3.4.1. Sample size selection

This study included 50 elderly patients with type 2 diabetes and conducted a 30-min experiment to explore the correlation between blood routine parameters and electrocardiogram characteristics. Sample size was determined based on statistical power (≥ 0.8), medium effect size (0.5), and significance level ($\alpha = 0.05$) to ensure data reliability while meeting experimental monitoring requirements and equipment capacity. This sample size can cover different levels of glucose control and complications, improving the applicability of results. The effects of blood glucose control on electrocardiogram characteristics were analyzed according to the level of HbA1c ($\leq 7\%$ vs. $> 7\%$).

Inclusion criteria: 1) Age $\geq$ 65 years; 2) Duration of diabetes $\geq$ 5 years; 3) no serious cardiovascular disease; 4) can cooperate with the experiment. Exclusion criteria: 1) Major surgery or acute infection within the last 6 months; 2) severe hepatic and renal insufficiency; 3) Take drugs that may interfere with the experiment.

3.4.2. Statistical analysis method

The mean, standard deviation, and range of routine blood and electrocardiogram features were calculated, and frequency and percentage were used to describe baseline features such as age, sex, and disease course of the sample. Pearson correlation was used to analyze the linear relationship between blood routine and ECG characteristics, and Spearman rank correlation was used for non-normal data. The relationship between ECG characteristics and blood routine indexes was analyzed by multiple regression model, confounding factors were controlled, and significant predictors were screened by stepwise regression. The differences between different blood glucose control groups were compared using the *T*-test. Time series analysis was performed on the 30-min monitoring data, using repeated measurement ANOVA to compare differences at different time points. Statistical significance was set at $P < 0.05$, and Bonferroni correction controlled for multiple comparison errors. *G**Power analysis showed that the sample size of 45 was sufficient, and 50 samples were included in this study to enhance robustness.

4. Analysis of experimental results

The study utilized the synergistic effect of AuNP and captured probes to achieve efficient detection of miRNAs. Moreover, the specific recognition ability of the sensor for biomarkers such as α2-M was enhanced by antibody modification. Meanwhile, the correlation between blood routine indexes and ECG features was explored using multiple linear regression modeling in conjunction with dynamic monitoring of ECG features. To ensure the reliability and stability of the experimental results, three independent repeated experiments will be conducted in this study. Each experiment was conducted under the same conditions, including the same equipment calibration, sample processing procedures, and data acquisition methods.

4.1. Sensitivity analysis

The study was conducted to condition the experimental environment to improve the testing performance of the biosensor. The optimized test results of the experimental conditions are shown in **Figure 2**.

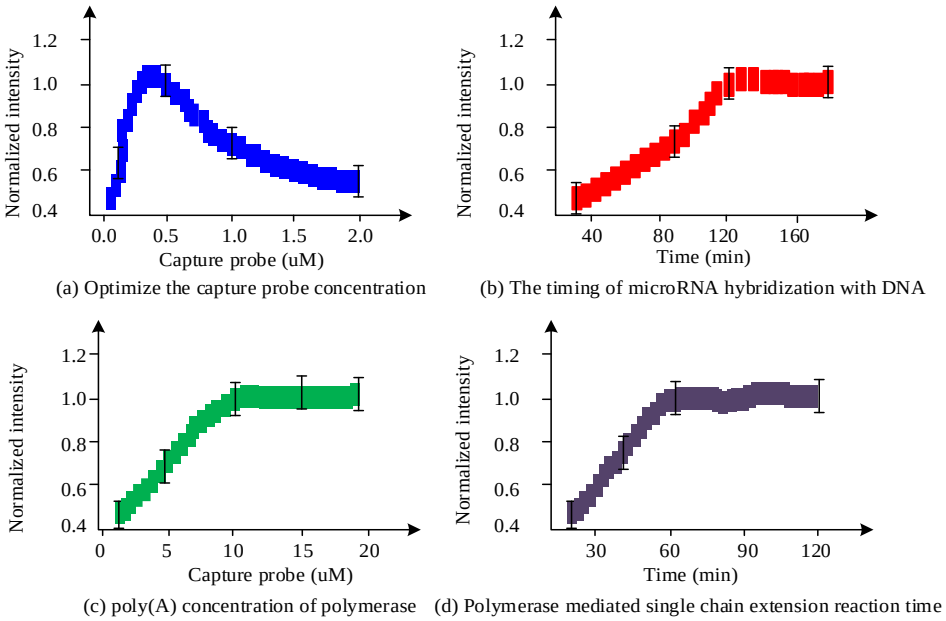

Figure 2. Optimal experimental conditions for biosensors.

In **Figure 2a**, the capture probe concentration had a significant effect on the signal intensity. The signal intensity peaked at 0.5 μm, and then too high concentration instead led to a decrease in the signal, which might be related to the increase in non-specific binding. In **Figure 2b**, the signal was gradually enhanced and stabilized around 120 min with the increase of reaction time, indicating that 120 min was the optimal hybridization reaction time. In **Figure 2c**, the signal was significantly enhanced with increasing polymerase concentration and approached saturation after 15 U/mL, suggesting that the optimal concentration was 15 U/mL. In **Figure 2d**, the extension reaction time was positively correlated with the signal intensity, and the signal tended to stabilize at 90 min, showing that the optimal extension time was 90 min. Based on the above optimal experimental conditions, the sensitivity detection results of the biosensor are shown in **Figure 3**.

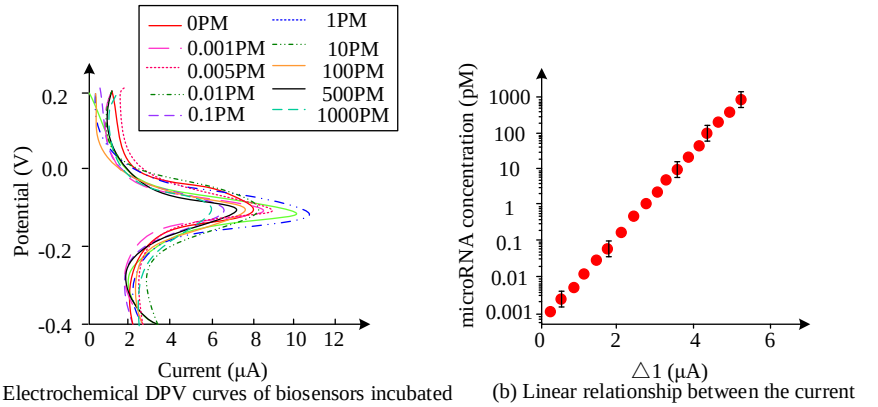

(a) Electrochemical DPV curves of biosensors incubated with different concentrations of microRNA (a~j: 0, 0.001, 0.005, 0.01, 0.1, 1, 10, 100, 500, 1000pM).

(b) Linear relationship between the current difference (AI) and the logarithm of microRNA concentration in the range 0.001-1000pm.

Figure 3. Sensitivity detection results of biosensor.

In **Figure 3a**, the DPV curves for different concentrations of miRNA showed that the signal peaks increased with the increase of miRNA concentration, and the current values gradually increased from about 3.90 μA at 0 pm to about 11.20 μA at 1000 pm. A significant correlation between concentration and signal was shown. Under the experimental conditions, the detection range covered 0.001–1000 pm, and the sensor had high sensitivity to low concentrations of miRNAs. **Figure 3b** displayed the linear relationship between miRNA concentration and current difference (ΔI) with a linear range of 0.001–1000 pm. The slope of the regression equation indicated that the sensor maintained good responsiveness over a wide concentration range. In addition, the standard error was small, indicating good reproducibility of the experimental results.

4.2. Selectivity, reproducibility, stability analysis

In order to verify the performance of the sensor in this study, the experiment compares it with the prior art in terms of anti-interference ability and cost effectiveness, and the results are shown in **Table 3**.

Table 3. Performance comparison results of different sensors.

Performance index	Sensor of this study	Optical sensors by Sani et al	RT-CGM system
Detection limit (μmol/L)	0.850	0.500	0.300
Data collection rate (times/s)	50.000	10.000	8.000
Detection accuracy increased by percentage	15.800	10.000	5.000
Anti-interference capability	high	In the	low
Cost-benefit ratio	1.000	0.800	0.500
Real-time monitoring capability	Strong	Medium	Strong

In **Table 3**, the sensor in this study is superior to the prior art in several performance indexes. The detection limit of 0.850 μmol/L is higher than the optical sensor of Sani et al., and the RT-CGM system, showing its high sensitivity to low concentrations of substances. The data collection rate is as high as 50 times/s, which is much higher than the other two technologies, ensuring the high efficiency of real-time monitoring. The percentage improvement in detection accuracy is also leading, reaching 15.8%, indicating higher accuracy. The anti-interference ability is strong, the

cost-benefit ratio is 1.000, which is superior to other technologies and shows better economy. To evaluate the performance of the biosensor, 20 cyclic voltammetric scans were performed. **Figure 4** shows the results of the stability test of the biosensor.

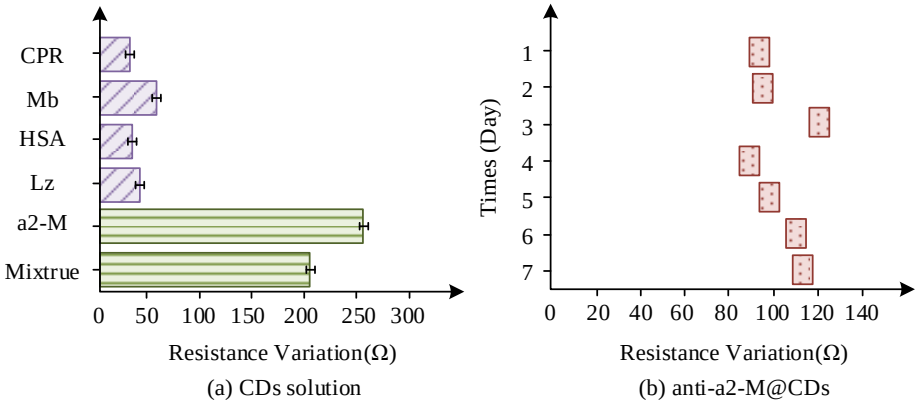

Figure 4. Stability test results of biosensor.

In **Figure 4a**, the resistance change of α2-M was significantly higher than that of other antigens, and the value of the resistance change was close to 250 Ω. It indicated that the sensor was more capable of recognizing α2-M specifically, while the response to other antigens and their mixtures was weaker, about 50 Ω. In **Figure 4b**, the resistance change of the sensor in response to α2-M had a small fluctuation range across days and the relative standard deviation (RSD) was 6.504%, indicating that the sensor had good long-term stability. The results verified the high specificity and good stability of the designed biosensor for α2-M with small fluctuation of values. **Figure 5** shows the effect of the biosensor employed in 30 min.

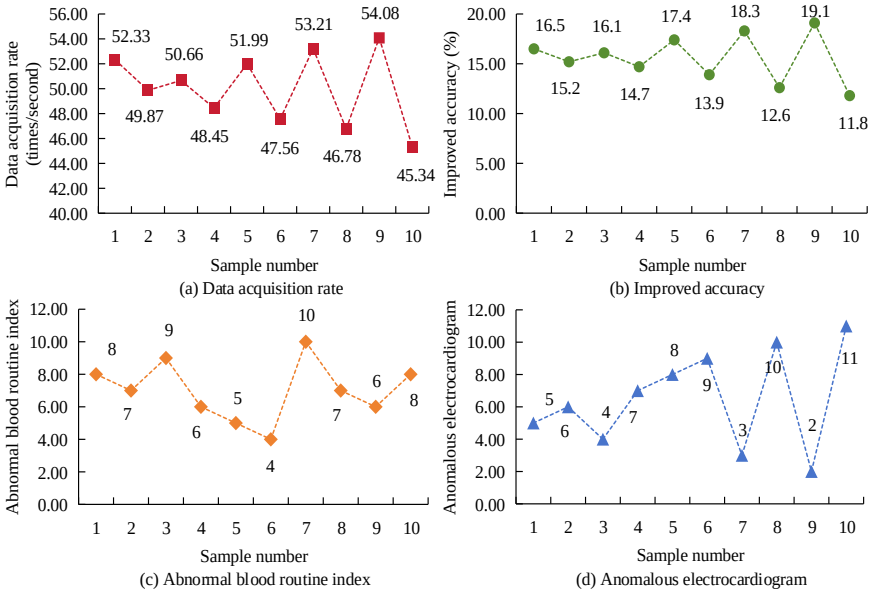

Figure 5. Effect of biosensor in 30 min.

In **Figure 5**, the acquisition rates of the biosensors ranges from 45.34 times/s to 54.08 times/s over a 30-min period, with a high average rate, indicating that the sensors have a strong real-time monitoring capability. The accuracy indicators (percentage)

were distributed between 11.8% and 19.1%, with some samples showing lower accuracy, which may be affected by biosignal interference or device calibration. The number of abnormalities in routine blood indicators ranged from 6 to 10 cases, while the samples with abnormal ECG characteristics were concentrated in the range of 2 to 11 cases, indicating that the detection of ECG abnormalities was more sensitive. Overall, the sensors showed some efficiency and stability in the rapid detection of blood and ECG index abnormalities.

4.3. Cell serum analysis

The surface properties of the biosensor functionalized by antibody modification were investigated by SEM characterization experiments, combined with EDS analysis and images, as shown in **Figure 6**.

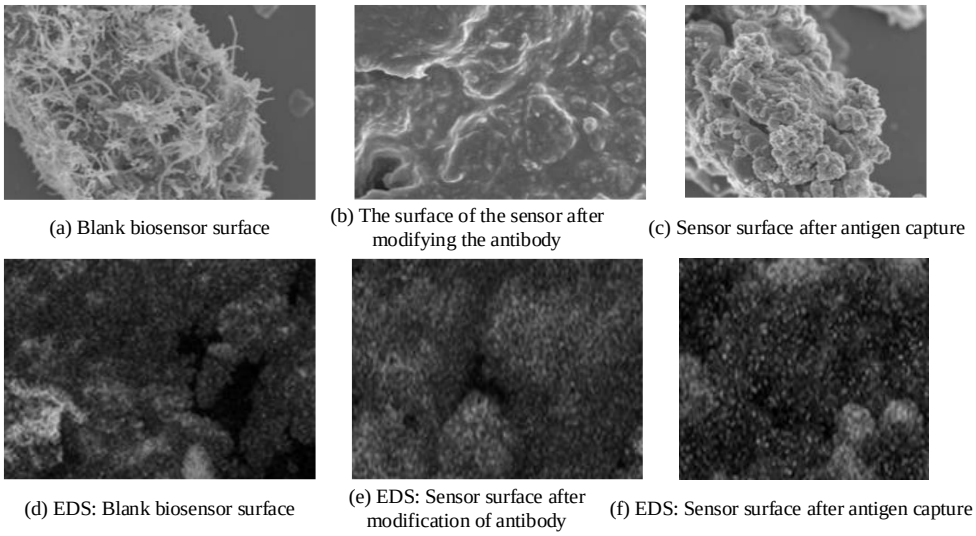

Figure 6. SEM and EDS characterization of biosensors.

In **Figure 6a–c**, SEM images of **Figure 6a** show that the blank surface was relatively flat and lacked significant features. In **Figure 6b**, after modifying the antibody, the surface morphology showed obvious granular changes, indicating successful immobilization of the antibody. In **Figure 6c**, after capturing the antigen, the surface became more complex, showing the process of antigen capture. Combined with the EDS images **Figure 6 d–f**, the distribution of elements such as C, N, and O could be visualized, further confirming the successful application of functionalized sensors in capturing antigens. By accurately modifying antibodies and capturing specific antigens, the sensor could realize efficient recognition of target biomarkers. Using the biosensor, the correlation results of detecting bilirubin levels with routine blood test results are shown in **Figure 7**.

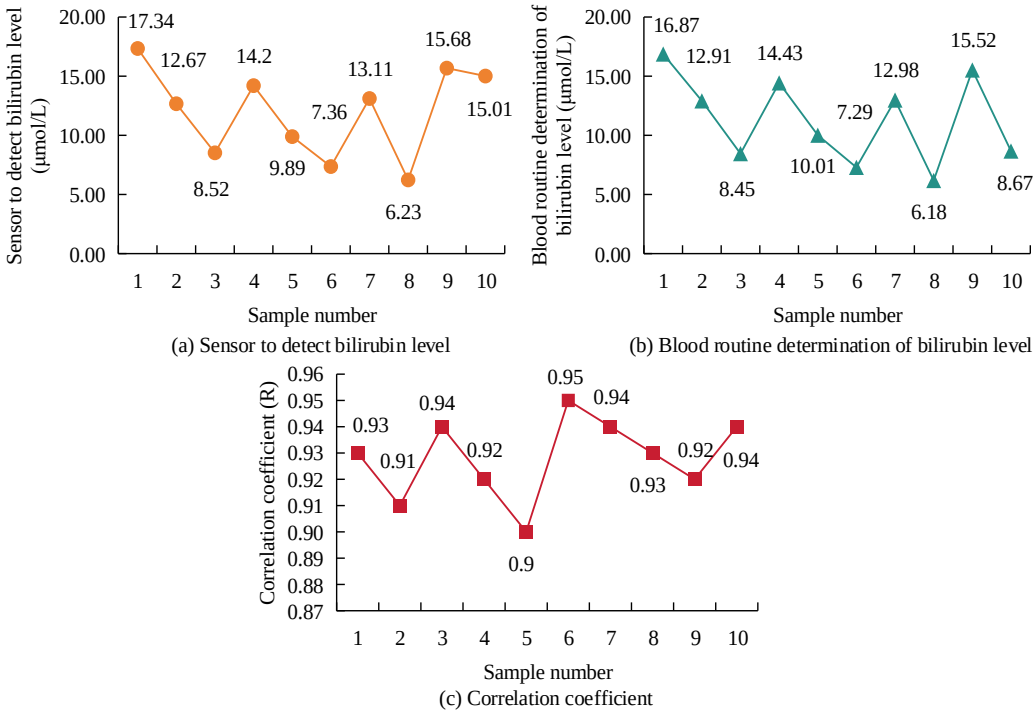

Figure 7. Correlation between bilirubin levels and blood routine test results.

In **Figure 7**, the correlation between the bilirubin levels detected using the biosensor and the results of routine blood tests was high. The values of bilirubin levels detected by the sensor and those detected by routine blood tests were close to each other in each sample, and the deviations were within reasonable limits. The difference was only 0.53 μmol/L in Sample 1 and 0.16 μmol/L in Sample 9, showing good agreement between the two assays. The *R* value of the correlation coefficient was between 0.90 and 0.95, which further proved that there was a significant positive correlation between the two. **Table 4** shows the detection and statistical results of the biosensors on the changes of leukocytes, bilirubin levels, and electrocardiogram characteristics in blood routine.

Table 4. Results of changes of leukocyte, bilirubin levels, and electrocardiogram characteristics.

Sample number	White blood cell count (× 109/L)	Bilirubin level (μmol/L)	Electrocardiogram characteristic change
1	7.05	15.23	Slight elevation of the ST segment
2	5.68	12.47	T-waves are low
3	8.12	18.56	The QT interval is prolonged
4	6.34	14.21	U-wave anomaly
5	4.97	11.39	normal
6	7.89	16.78	T-wave inversion
7	6.73	13.65	St-segment depression
8	5.29	10.98	normal
9	8.45	19.02	T-wave change
10	7.21	15.43	The QT interval is prolonged

In **Table 4**, the white blood cell count 109/L ranged from 4.97/L to 8.45/L. The

majority of samples were within the normal range, reflecting the stability of the immune system. Bilirubin levels ranged from 12.27 μmol/L to 19.86 μmol/L, with some samples on the high side, suggesting that mild abnormalities in liver function may exist. In terms of electrocardiographic features, cardiac abnormalities such as ST-segment changes, T-wave abnormalities, and QT interval prolongation were more prominent. This indicated that myocardial ischemia or cardiac conduction system problems may exist in some samples. The levels of leukocytes and bilirubin in some samples showed some correlation with ECG, which could suggest the combined effect of inflammation or cardiac metabolic abnormalities. To further explore the correlation between bilirubin levels and ECG characteristics, Pearson correlation coefficient and corresponding *T*-test were used, and the results were shown in **Table 5**.

Table 5. Correlation between bilirubin levels and ECG characteristics.

Sample number	Bilirubin level (μmol/L)	ECG characteristic change	Correlation coefficient (r)	*t*	*P*
1	15.23	0.5	0.87	5.67	< 0.001
2	12.47	0.3			
3	18.56	0.8			
4	14.21	0.4			
5	11.39	0.2			
6	16.78	0.7			
7	13.65	0.3			
8	10.98	0.1			
9	19.02	0.9			
10	15.43	0.6			

In **Table 5**, there is a significant positive correlation between bilirubin levels and changes in ECG characteristics, and Pearson correlation coefficient is 0.87, indicating a strong linear relationship between the two. A t value of 5.67, corresponding to $P < 0.001$, is much lower than the usual significance level of 0.05, suggesting that this association is not due to chance. These results suggest that elevated bilirubin levels may be associated with changes in ECG characteristics, providing a new biomarker for cardiovascular risk assessment in older patients with diabetes.

5. Conclusion

To investigate the effect of dynamic monitoring of blood routine on the electrocardiogram characteristics of geriatric diabetes mellitus patients and to develop a real-time detection system based on electrochemical biosensors, this study was conducted to detect biomarkers such as bilirubin and α2-M in the blood of patients by designing a novel sensor. It was also combined with multiple linear regression model to analyze the correlation between blood and ECG features. Layer-by-layer self-assembly technology was used to construct the high-sensitivity sensor, optimize its sensitivity, selectivity, and stability, and verify its application effect in real samples using cellular serum analysis. The results revealed that the developed electrochemical biosensor had significant efficacy in detecting biomarkers in patients with geriatric diabetes mellitus. The correlation coefficient between the sensor's detection of

bilirubin and routine blood results was as high as 0.95, and the detection limit was 0.85×10^9/L, with an improved accuracy of 15.8%, which was significantly better than the traditional method. The linear range of miRNA detection was 0.001–1000 pm, and the current response was positively correlated with the concentration, indicating that the sensor had excellent sensitivity and wide dynamic detection range. In addition, the sensor's good stability in detecting α2-M with an Relative Standard Deviation (RSD) of only 6.5% confirmed its reliability for long-term monitoring. These data strongly demonstrated the potential of the sensor for clinical applications in the management of geriatric diabetes mellitus, especially in real-time monitoring and early diagnosis. The sensor for α2-M detection was only 6.5%, showing good long-term stability.

The sensor developed by the research has excellent performance in real-time monitoring physiological indicators of patients with chronic diseases, especially in the measurement of heart rate and blood oxygen saturation, and the error rate is significantly lower than that of prior art. Its low power consumption and wireless transmission design make it advantageous in long-term monitoring. However, there are still limitations: first, the anti-interference ability needs to be improved, especially in high humidity or strong electromagnetic environment; Second, the sample size is limited and larger scale clinical verification is needed. Third, the cost is higher, which may affect the promotion. Future research will focus on optimizing anti-interference performance, improving materials and algorithms, and exploring disease monitoring such as diabetes and hypertension, while reducing costs and incorporating artificial intelligence to promote personalized health management.

Author contributions: Conceptualization, LZ; methodology, YY; software, NM; data curation, YY; writing—original draft preparation, LZ; writing—review and editing, NM. All authors have read and agreed to the published version of the manuscript.

Ethical approval: Not applicable.

Conflict of interest: The authors declare no conflict of interest.

References

1. Ortiz-Martínez M, González-González M, Martagón AJ, et al. Recent Developments in Biomarkers for Diagnosis and Screening of Type 2 Diabetes Mellitus. Current Diabetes Reports. 2022; 22(3): 95-115. doi: 10.1007/s11892-022-01453-4
2. Renard E, Riveline J, Hanaire H, et al. Reduction of clinically important low glucose excursions with a long-term implantable continuous glucose monitoring system in adults with type 1 diabetes prone to hypoglycaemia: the France Adoption Randomized Clinical Trial. Diabetes, Obesity and Metabolism. 2022; 24(5): 859-867. doi: 10.1111/dom.14644
3. Saha T, Del Caño R, Mahato K, et al. Wearable Electrochemical Glucose Sensors in Diabetes Management: A Comprehensive Review. Chemical Reviews. 2023; 123(12): 7854-7889. doi: 10.1021/acs.chemrev.3c00078
4. Gubitosi-Klug RA, Braffett BH, Bebu I, et al. Continuous Glucose Monitoring in Adults With Type 1 Diabetes With 35 Years Duration From the DCCT/EDIC Study. Diabetes Care. 2022; 45(3): 659-665. doi: 10.2337/dc21-0629
5. Sani MH, Khosroabadi S. A Novel Design and Analysis of High-Sensitivity Biosensor Based on Nano-Cavity for Detection of Blood Component, Diabetes, Cancer and Glucose Concentration. IEEE Sensors Journal. 2020; 20(13): 7161-7168. doi: 10.1109/jsen.2020.2964114
6. Marigliano M, Piona C, Mancioppi V, et al. Glucose sensor with predictive alarm for hypoglycaemia: Improved glycaemic control in adolescents with type 1 diabetes. Diabetes, Obesity and Metabolism. 2024; 26(4): 1314-1320. doi: 10.1111/dom.15432

7. Levy CJ, Kudva YC, Ozaslan B, et al. At-Home Use of a Pregnancy-Specific Zone-MPC Closed-Loop System for Pregnancies Complicated by Type 1 Diabetes: A Single-Arm, Observational Multicenter Study. Diabetes Care. 2023; 46(7): 1425-1431. doi: 10.2337/dc23-0173
8. Lazar MA, Magnuson MA, Kaestner KH. Franz Matschinsky, MD (1931–2022): Paragon of Scientific Rigor and Curiosity Who Discovered Glucokinase as the Pancreatic Glucose Sensor. Diabetes. 2022; 71(10): 2078-2083. doi: 10.2337/dbi22-0017
9. Schiavon M, Galderisi A, Basu A, et al. A New Index of Insulin Sensitivity from Glucose Sensor and Insulin Pump Data: In Silico and In Vivo Validation in Youths with Type 1 Diabetes. Diabetes Technology & Therapeutics. 2023; 25(4): 270-278. doi: 10.1089/dia.2022.0397
10. Riahi Y, Kogot-Levin A, Kadosh L, et al. Hyperglucagonaemia in diabetes: altered amino acid metabolism triggers mTORC1 activation, which drives glucagon production. Diabetologia. 2023; 66(10): 1925-1942. doi: 10.1007/s00125-023-05967-8
11. Nagarajan A, Sethuraman V, Sasikumar R. Non-enzymatic electrochemical detection of creatinine based on a glassy carbon electrode modified with a Pd/Cu2O decorated polypyrrole (PPy) nanocomposite: an analytical approach. Analytical Methods. 2023; 15(11): 1410-1421. doi: 10.1039/d3ay00110e
12. Sherr JL, Heinemann L, Fleming GA, et al. Automated Insulin Delivery: Benefits, Challenges, and Recommendations. A Consensus Report of the Joint Diabetes Technology Working Group of the European Association for the Study of Diabetes and the American Diabetes Association. Diabetes Care. 2022; 45(12): 3058-3074. doi: 10.2337/dci22-0018
13. Matejko B, Juza A, Kieć-Wilk B, et al. One-Year Follow-Up of Advanced Hybrid Closed-Loop System in Adults with Type 1 Diabetes Previously Naive to Diabetes Technology: The Effect of Switching to a Calibration-Free Sensor. Diabetes Technology & Therapeutics. 2023; 25(8): 554-558. doi: 10.1089/dia.2023.0059
14. Seget S, Rusak E, Polanska J, et al. Prospective Open-Label, Single-Arm, Single-Center Follow-Up Study of the Application of the Advanced Hybrid Closed Loop System in Well-Controlled Children and Adolescents with Type 1 Diabetes. Diabetes Technology & Therapeutics. 2022; 24(11): 824-831. doi: 10.1089/dia.2022.0148
15. Kong YW, Venkatesh N, Paldus B, et al. Upload and Review of Insulin Pump and Glucose Sensor Data by Adults with Type 1 Diabetes: A Clinic Audit. Diabetes Technology & Therapeutics. 2022; 24(7): 531-534. doi: 10.1089/dia.2021.0558
16. Lekshmi MS, & Suja KJ. Enhanced acetone detection using ZnS-NiO heterojunction sensor for diabetes detection. Ceramics International. 2024; 50(13): 23577-23585. doi: 10.1016/j.ceramint.2024.04.080
17. Knies M, Teske E, Kooistra H. Evaluation of the FreeStyle Libre, a flash glucose monitoring system, in client-owned cats with diabetes mellitus. Journal of Feline Medicine and Surgery. 2022; 24(8): e223-e231. doi: 10.1177/1098612x221104051
18. Korgaonkar J, Tarman AY, Ceylan Koydemir H, et al. Periodontal disease and emerging point-of-care technologies for its diagnosis. Lab on a Chip. 2024; 24(14): 3326-3346. doi: 10.1039/d4lc00295d
19. Sun WH, Ye B. Fresh hetero-metallic compound as luminescent sensor for detection of CS2 and inhibitory activity on children diabetes. Journal of Fluorescence. 2022; 32(4): 1435-1441. doi: 10.1007/s10895-022-02943-0
20. Khoshbin Z, Shakour N, Iranshahi M, et al. Aptamer-based Biosensors: Promising Sensing Technology for Diabetes Diagnosis in Biological Fluids. Current Medicinal Chemistry. 2023; 30(30): 3441-3471. doi: 10.2174/0929867329666220829150118